Detection and Classification of Soft Tissues using Complex Shear Modulus Estimation and Decision Tree Algorithm

Luong Quang Hai, Nguyen Manh Cuong
Le Qui Don Technical University
Ha Noi, Viet Nam
{luonghai, nmcuong}@mta.edu.vn

Tran Duc-Tan
VNU University of Engineering & Technology
Ha Noi, Viet Nam
tantd@vnu.edu.vn

***Abstract*— Complex shear modulus (CSM) estimation is an effective facility to analyze the mechanical properties of tissues in terms of elasticity and viscosity. CSM can be used to detect and classify some kinds of soft tissues. However, the challenge is the estimation accuracy, and computational complexity. In this paper, we propose a 2D CSM estimation and classification of soft tissues based on the Extended Kalman Filter (EKF) and the Decision Tree (DT) algorithm. EKF is used to estimate the CSM at each spatial point by exploiting the shear wave propagation. A simple and effective decision tree algorithm is then developed for the classification of three kinds of tissues. Simulated experiment and performance study are carried out to confirm the quality of the proposed method.**

Keywords— Shear wave elasticity imaging; complex shear modulus; extended Kalman filter; decision tree.

I. INTRODUCTION

Estimation of tissue elasticity and viscosity has emerged as an important advance in biomedical imaging and tissue classification. Firstly, shear wave elasticity imaging (SWEI) is only used to provide additional information in the diagnosis [1]. After that, in 2013, Gennission et al. have shown that SWEI has important advantages compared to other techniques in terms of quantitativity, and elasticity contrast [2]. In 2014, Ferraioli et al. proved that they can apply shear wave elastography to evaluate the liver fibrosis [3]. Up to now, the commercialized SWEI devices are avaible on the market [4]. However, the devices which provide both the tissue's elasticity and viscosity are rare.

We need to measure shear wave propagation velocities within the tissues at a certain or some frequencies to find this tissues' properties. It can be done by applying acoustic radiation, surface vibration, or deep vibration as the mechanical force [5]-[9]. In [10], Orescanin et al. created the shear wave propagation by using a vibrating needle. The direct algebraic Helmholtz inversion can be used to directly compute the CSM [11]. However, the disadvantage of this method is that it takes a long processing time and easily affect by noise. This limitation is solved by using a Bayesian approach that provides a better estimate of the velocity in low SNR [12]. The limitation of [12] is that it can only work with homogeneous tissues only. In our recent work [13], we extended the method in [12] to heterogeneous media. Specifically, we applied the maximum likelihood ensemble filter (MLEF) [14] for more effective estimation of the CSM.

Recently methods proposed for automatic classification are based on different machine learning algorithms such as decision-trees, k-means, HMMs, and SVM. These techniques have been also applied to differentiate some tissues, lesions, tumors, etc [17][18][19]. In this paper, we exploit the advantages of such: 1) the model based estimation using EKF to compute the CSM and 2) the decision-tree (DT) algorithm to classify three kinds of soft tissues in livers. In detail, our DT algorithm can distinguish among normal, substantial fibrosis, and cirrhosis in livers. Simulated experiment and performance study are carried out to confirm the quality of the proposed method. The result indicates that this study helps improve the quality of estimation and classification.

II. MATERIAL AND METHOD

A. Detection of Tumors in Soft Tissue

Fig. 1 schematically shows the configuration of the shear wave estimation system. A mechanical actuator and a stainless-steel needle are used to generate a vertical vibration at a certain frequency ($100 \leq f \leq 500$ Hz). The shear wave is then propagated in tissue and the particle velocity is measured by a Doppler device.

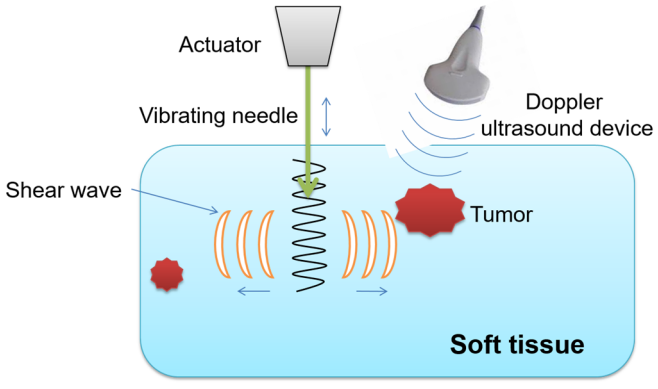

Fig. 1. Excitation and acquisition of the shear wave estimation system.

978-1-5386-2896-6/17/$31.00 ©2017 IEEE

Quantitative information about soft tissue mechanical properties can be represented by complex shear modulus (CSM) [1],

$$\mu = \mu_1 - i\omega\mu_2, \quad (1)$$

where μ_1 is the elastic shear constant and μ_2 is the dynamic viscosity constant defined the Kelvin-Voigt model.

The region of interest (ROI) consists of the reconstructing objects (if any) in a 2-D space (see Fig. 2). A ray scanning technique is used to cover the ROI: the area is scanned by varying the angle from 0° to 90° in the step of 1° in order to create 91 rays. Note that, the particle velocity is measured at each spatial point in each ray by the Doppler device. In order to detect the tumors by exploiting the mechanical properties of tissues in term of elasticity and viscosity, two object functions can be defined by

$$O_1(\vec{r}) = \begin{cases} \mu_1 - \mu_1^0, \vec{r} \in abnormal\ tissue \\ 0, \quad if\ not \end{cases}, \quad (2)$$

and

$$O_2(\vec{r}) = \begin{cases} \omega(\mu_2 - \mu_2^0), \vec{r} \in abnormal\ tissue \\ 0, \quad if\ not \end{cases}, \quad (3)$$

where μ_1 and μ_2 are the elasticity and viscosity of the abnormal tissue (if any), μ_1^0 and μ_2^0 are the elasticity and viscosity of the normal tissue, and ω is the angular frequency ($\omega = 2\pi f$).

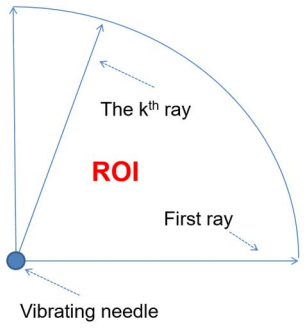

Fig. 2. Ray scanning in the ROI.

In practice, we cannot estimate CSM directly. CSM is derived from the wave number k_s and attenuation α coefficients [2],

$$\mu_1 = \frac{\rho\omega^2(k_s^2 - \alpha^2)}{(k_s^2 + \alpha^2)^2}, \quad \mu_2 = \frac{2\rho k_s \alpha}{(k_s^2 + \alpha^2)^2} \quad (4)$$

The detail of model-based estimation of the wave number k_s and attenuation α coefficients using Extended Kalman Filters can be found in [15]. An effective EKF is designed to estimate the wave number k_s and attenuation α at each point of a line in tissues which belongs to ROI. After this step, we obtained a cloud of points in ROI and the corresponding wave number k_s and attenuation α coefficients. Consequently, CSM coefficient is computed by using Equ. (4). Finally, the object functions are reconstructed by using Equs. (2) and (3).

B. *Classification of Soft Tissue*

Liver fibrosis is not a disease, and it's caused by the imbalance between the collagen fiber synthesis and decomposition [16]. Fibrosis and cirrhosis are different, but cirrhosis are often developed from fibrosis. Up to now, a liver biopsy is still the most reliable facility to diagnose the fibrosis levels. In this study, we develop a decision-tree (DT) as shown in Fig. 3 to classify three states in livers: normal, substantial fibrosis, and cirrhosis. In this flow chart, we introduce to use three thresholds: threshold_A, threshold_B, and threshold_C. Because the cirrhosis is always 'harder' than the other, thus, the elasticity object function O_1(r) is firstly used to determine if there is a cirrhosis at the position r by using Threshold_A. Moreover, it would be confirmed there is a cirrhosis if the viscosity O_2(r) > Threshold_B. To distinguish between the substantial fibrosis and normal liver tissue, we need concern both the elasticity and viscosity object functions concurrently. The substantial fibrosis is determined if $|O_1(r)+i.O_2(r)|$ > Threshold_C.

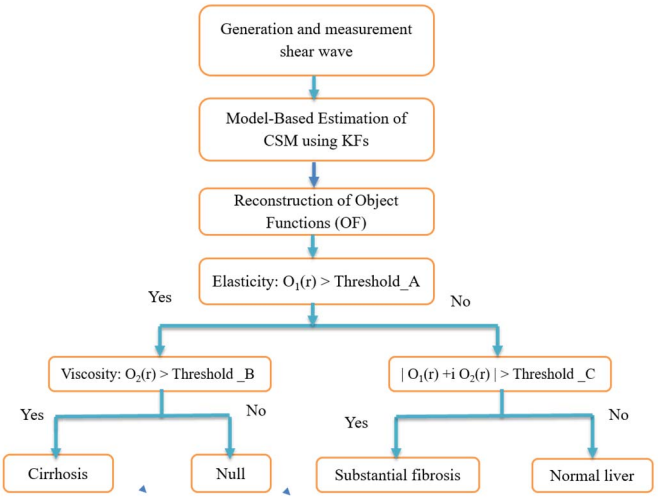

Fig. 3. Tumor classification using the proposed decision tree algorithm

III. SIMULATION AND RESULTS

In this paper, we examine the proposed work with a simulated scenario wherein three different kinds of tissues with the corresponding elasticity and viscosity as shown in Table 1. These values are referred from the work [16].

TABLE 1. Parameters of some typical states of liver

	Types	Shear elasticity (kPa)	Shear viscosity (Pa.s)
1	Patients with substantial fibrosis	2.56	2.27
2	Patients with cirrhosis	4.68	5.19
3	Normal human liver	2.06	1.72

The needle with the diameter of 1.5 mm was set to vibrate with frequency $f_0 = 100$ Hz. The data were also collected over 43 spatial locations, distance between two continuous point is 0.3 mm, the sampling frequency is 10 kHz, and 500

samples are acquired at each spatial location. In our work, threshold_A, threshold_B, and threshold_C are chosen at 3.620 kPa, 2.344 kPa and 2.828 kPa, respectively.

Fig. 4 shows the ideal elasticity object function O_1 where the vibrating needle is set the origin point. Values of three tissues in this figure are mentioned in Table 1. It can be seen that the elasticity difference between the fibrosis and normal liver is not clearly shown.

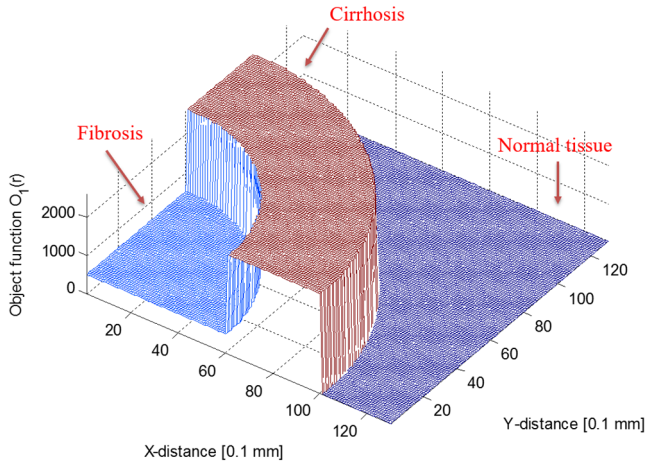

Fig. 4. The elasticity object function $O_1(r)$

Fig. 5 shows the reconstructed elasticity object function $\widehat{O_1}$ using the proposed work. Although there are ripples on the surface, the reconstructed object function traced the ideal one very well. The ripples are caused by the added noise and the imperfect of the reconstructed model. It is difficult to distinguish between the fibrosis and normal liver due to the ripples. Also in Fig. 5, we can see that the ray scanning technique could not cover all the square area of 12.6×12.6 mm^2. The region of interest (ROI) is just a sector with the radius of 12.6 mm.

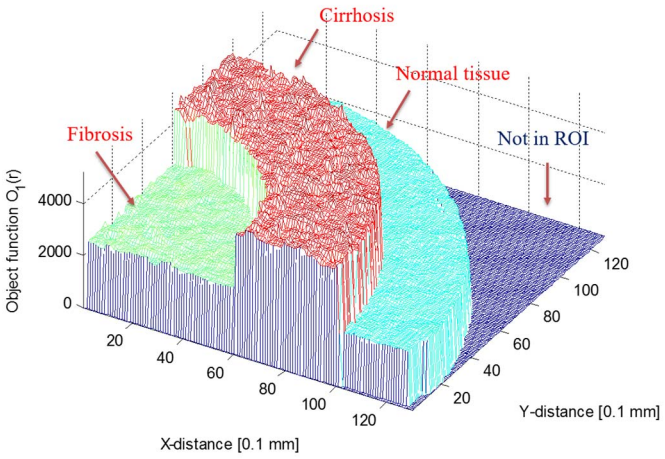

Fig. 5. The reconstructed elasticity object function $O_1(r)$ which was added by the elasticity of normal liver tissue (i.e. 2.06 kPa) to show tissues are in and not in ROI.

Figures 6.a and 6.b show the estimation results for the wave number and attenuation coefficients along the 60th ray at SNR = 30 dB. It can be seen that a sudden change of the wave number happens at the distances of 6 mm (between the fibrosis and the cirrhosis) and 100 mm (between the cirrhosis and the normal tissue). This changing is also found in Figs. 4 and 5. In Figs. 6a and 6b, the estimated wave number and attenuation coefficients can track the ideal ones very well. However,the ripples in the attenuation estimation are larger than the one in the wave number estimation. After we estimated the wave number and attenuation coefficients, the elasticity and the viscosity can be computed by using Equ. (4). Consequently, the object functions $O_1(r)$ and $O_2(r)$ are finally reconstructed.

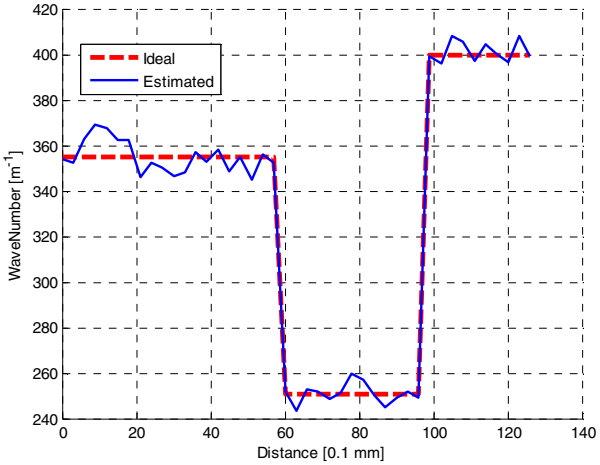

(a) Estimation of k_s

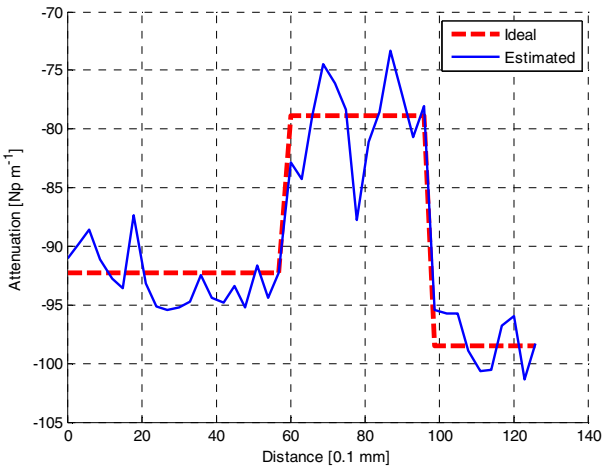

(b) Estimation of α

Fig. 6. Estimation of wave number and attenuation coefficient along the 60th ray.

Appling the threshold_A and threshold_B to the DT algorithm as shown in Fig. 3, it is easy to separate cirrhosis locations from the group of the fibrosis and the normal tissue. However, if we only concern to $\hat{O}_1$ or $\hat{O}_2$ for the classification of the fibrosis and normal tissue, the performance would not be good enough. Thus, in order to distinguish between the fibrosis and

normal liver, the magnitude of $|\hat{O}_1 + i \times \hat{O}_2|$ is computed, then the threshold_C is applied (see Fig. 3). The reason is that the magnitude of $|\hat{O}_1 + i \times \hat{O}_2|$ can amplify the difference between the fibrosis and normal tissue. Fig. 7 shows the reconstructed CSM image which can point out exactly the locations of soft tissues (fibrosis, cirrhosis, and normal liver) in ROI.

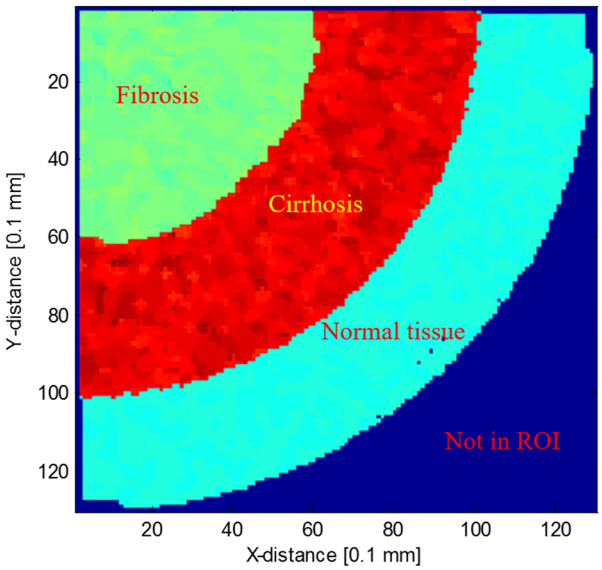

Fig. 7. CSM image which is able to clarify show three different kinds of soft tissues (fibrosis, cirrhosis, and normal liver) in ROI.

IV. CONCLUSIONS

Our work has shown that shear wave estimation can be used to detect and classify some important states of tissues. Simulation scenarios of reconstruction of object functions in elasticity and viscosity were conducted to prove the good performance of this method. The simple DT classification algorithm was useful in classification of estimated patterns. Hence it can automatically detect the health problem. In the future work, we will consider how to enhance the classification performance by combining the DT algorithm with SVM. The scheme can be further developed by 3D reconstruction and experiment.

ACKNOWLEDGMENT

This work was supported by the Asia Research Center (ARC), Vietnam National University under Grant "Tumor detection using shear wave imaging". The analysis and write-up were carried out as a part of the first author's PhD study.

REFERENCES

[1] A. P. Sarvazyan, O. V. Rudenko, S. D. Swanson, J. B. Fowlkes, and S. Y. Emelianov, "Shear wave elasticity imaging: a new ultrasonic technology of medical diagnostics," Ultrasound in medicine & biology, vol. 24, no. 9, pp. 1419–1435, 1998.

[2] J.-L. Gennisson, T. Deffieux, M. Fink, and M. Tanter, "Ultrasound elastography: principles and techniques," Diagnostic and interventional imaging, vol. 94, no. 5, pp. 487–495, 2013.

[3] G. Ferraioli, P. Parekh, A. B. Levitov, and C. Filice, "Shear wave elastography for evaluation of liver fibrosis," Journal of Ultrasound in Medicine, vol. 33, no. 2, pp. 197–203, 2014.

[4] Skerl, K., Cochran, S., & Evans, A. (2017). First step to facilitate long-term and multi-centre studies of shear wave elastography in solid breast lesions using a computer-assisted algorithm. International Journal of Computer Assisted Radiology and Surgery, 1-10.

[5] Chen S, Fatemi M, Greenleaf JF (2007). Real time shear velocity imaging using sonoelastograpgic techniques. Ultrasound Medical Biology, 115:2781-2785.

[6] Nightingale K, McAleavey S, Trahey G (2003). Shear-wave generation using acoustic radiation force: in vivo and ex vivo results. Ultrasound in Medicine and Biology, 29:1715-1738.

[7] Kanai MH (2009). Propagation of vibration caused by electrical excitation in the normal human heart. Ultrasound Medical Biology, 35:936-948.

[8] Orescanin M, Insana MF (2011). 3-D FDTD simulation of shear waves for evaluation of complex modulus imaging. IEEE Trans. Ultrasonics, Ferroelectrics, and Frequency Control, 58:389-398.

[9] Denis, M., Gregory, A., Bayat, M., Fazzio, R. T., Whaley, D. H., Ghosh, K., and Alizad, A. (2016). Correlating Tumor Stiffness with Immunohistochemical Subtypes of Breast Cancers: Prognostic Value of Comb-Push Ultrasound Shear Elastography for Differentiating Luminal Subtypes. PloS one, 11(10), e0165003.

[10] Orescanin M, Insana MF (2010). Shear Modulus Estimation With Vibrating With Needle Stimulation. IEEE Trans. Ultrasonics, Ferroelectrics, and Frequency Control, 57:1358-1367.

[11] Oliphant, T. E., Kinnick, R. R., Manduca, A., Ehman, R. L., & Greenleaf, J. F. An error analysis of Helmholtz inversion for incompressible shear, vibration elastography with application to filter-design for tissue characterization. In Ultrasonics Symposium, 2000 IEEE, Vol. 2, pp. 1795-1798.

[12] Orescanin M, Insana MF (2010). Model-based complex shear modulus reconstruction: A Bayesian approach. IEEE Int'l Ultrasonics Symposium, pp. 61-64.

[13] T. Tran-Duc, Y. Wang, N. Linh-Trung, M. N. Do, and M. F. Insana, "Complex Shear Modulus Estimation Using Maximum Likelihood Ensemble Filters," in 4th International Conference on Biomedical Engineering in Vietnam. Springer Berlin Heidelberg, 2013, pp. 313–316.

[14] Zupanski, M (2005). Maximum Likelihood Ensemble Filter: Theoretical Aspects. Monthly Weather Review, 133:1710-1726.

[15] Luong, Q. H., Nguyen, M. C., & Tan, T. D. A frequency dependent investigation of complex shear modulus estimation, International Conference on Advances in Information and Communication Technology, Springer International Publishing, 2016, pp. 31-40.

[16] Laurent Huwart, Frank Peeters, Ralph Sinkus, Laurence Annet, Najat Salameh, Leon C. ter Beek, Yves Horsmans, and Bernard E. Van Beers, Liver fibrosis: non-invasive assessment with MR elastography, NMR in biomedicine, 2006, vol. 19, pp. 173–179.

[17] Veyrieres, J. B., Albarel, F., Lombard, J. V., Berbis, J., Sebag, F., Oliver, C., & Petit, P. (2012). A threshold value in Shear Wave elastography to rule out malignant thyroid nodules: a reality?. European journal of radiology, vol. 81(12), pp. 3965-3972.

[18] Xiao, Y., Zeng, J., Qian, M., Zheng, R., & Zheng, H. (2013, July). Quantitative analysis of peri-tumor tissue elasticity based on shear-wave elastography for breast tumor classification. 35th Annual International Conference of the IEEE Engineering in Medicine and Biology Society (EMBC), 2013, pp. 1128-1131

[19] Olgun, D. Ç., Korkmazer, B., Kılıç, F., Dikici, A. S., Velidedeoğlu, M., Aydoğan, F., and Yılmaz, M. H. (2014). Use of shear wave elastography to differentiate benign and malignant breast lesions. Diagnostic and Interventional Radiology, vol. 20(3), p. 239.